frontiers | Frontiers in Earth Science

ORIGINAL RESEARCH
published: 26 April 2022
doi: 10.3389/feart.2022.861005

Paleoclimate Variations Spanning the Past 29–4 Ma Inferred From Lipid Biomarkers and Carbon Isotopes in the Linxia Basin, Northeast Tibetan Plateau

Gen Wang[1,2], Zhifu Wei[1,2], Ting Zhang[1,2], Wei He[1,2], Xueyun Ma[1,2], Xiaoli Yu[1,2] and Yongli Wang[3]**

[1]Northwest Institute of Eco-Environment and Resources, Chinese Academy of Sciences, Lanzhou, China, [2]Key Laboratory of Petroleum Resources, Lanzhou, China, [3]Key Laboratory of Cenozoic Geology and Environment, Institute of Geology and Geophysics, Chinese Academy of Sciences, Beijing, China

OPEN ACCESS

Edited by:
David K. Wright,
University of Oslo, Norway

Reviewed by:
Fei Wang,
Lanzhou University, China
Zhongshi Zhang,
China University of Geosciences Wuhan, China

***Correspondence:**
Yongli Wang
ylwang@mail.iggcas.ac.cn
Zhifu Wei
weizf@lzb.ac.cn

Specialty section:
This article was submitted to Quaternary Science, Geomorphology and Paleoenvironment, a section of the journal Frontiers in Earth Science

Received: 24 January 2022
Accepted: 30 March 2022
Published: 26 April 2022

Citation:
Wang G, Wei Z, Zhang T, He W, Ma X, Yu X and Wang Y (2022) Paleoclimate Variations Spanning the Past 29–4 Ma Inferred From Lipid Biomarkers and Carbon Isotopes in the Linxia Basin, Northeast Tibetan Plateau. Front. Earth Sci. 10:861005. doi: 10.3389/feart.2022.861005

Thick and continuous deposits in the Linxia Basin, located in the landing area of westerlies and monsoons, offer a good opportunity for understanding the climatic evolution and tectonic activities. However, detailed paleoclimate reconstruction based on lipid biomarkers was rare, which limited our further knowledge, even though there were some relevant reports regarding pollen assemblages, microbial communities. In the present study, we conducted systematic analyses on the lipid biomarkers and carbon isotope values of the sediments, in an effort to reconstruct the evolution history of paleoclimate and figure out the potential driving mechanism. Our results showed that the organic matter was from mixed sources including lower organisms and terrestrial higher plants. The organic matter sources varied in response to the change of paleoclimate conditions as revealed by the lipid-derived proxies and organic carbon isotopes. Significant climatic events like late Oligocene Warming, Mid-Miocene Climatic Optimum and aridification at ~8.5 Ma were observed throughout the sequence. Our results further indicated that the paleoclimate conditions in the study area primarily followed the pace of long-term global cooling, and the aridification at ~8.5 Ma was associated with the uplift of the Tibetan Plateau.

Keywords: late oligocene, n-alkanes, organic matter, stable organic carbon isotopes, aridification

INTRODUCTION

The increasing research hotspots of global environment and climate change has recently received a great attraction. Especially since the late Cenozoic, a series of major geological events have taken place on the earth, resulting in great changes in global climate and environment, such as global cooling (Miller et al., 1987; Miller et al., 1991; Zachos et al., 2001; Molnar et al., 2010; Haider et al., 2013; Zhuang et al., 2014; Kern et al., 2016), the aridity in north America and Asia (Ruddiman and Kutzbach, 1989; Manabe and Broccoli, 1990; Kutzbach et al., 1993; Rea et al., 1998; Wu et al., 2007; Wan et al., 2010; Tang et al., 2011; Kita et al., 2014; Jia et al., 2015), formation of the Asian monsoon (Quade et al., 1989; Li, 1995; An et al., 2001; Liu et al., 2008; Miao et al., 2011; Miao et al., 2012; Miao et al., 2013b; Liu et al., 2013; Li et al., 2014; Sun et al., 2014; Liu et al., 2015). Among these geological

events, the aridity in North America and Asia is a major scientific problem, which has the most profound and direct impact on human living environment. As the largest temperate arid zone in the world, the onset time, evolution sequence, formation process and driving mechanism of aridity in inland Asia are the research hotspots of environmental change in the Northern Hemisphere of Cenozoic era.

In terms of the development trend of inland aridity in Asian, the key scientific problem to be resolved is to reveal the onset time, evolution sequence, formation process of inland aridity in Asian (Sun and Wang, 2005), so as to explore its relationship with the driving mechanism (Boos and Kuang, 2010; Shi et al., 2011; Miao et al., 2012; Li et al., 2014). There have been different views on the driving mechanism of the evolution of Asian inland aridity in the late Cenozoic. At present, it is mainly reflected in three aspects: the uplift of the Tibet Plateau, the global cooling of the Cenozoic and the retreat of the Paratethys Sea. Previous studies have shown that the uplift of the Tibetan Plateau, the global cooling of the Cenozoic (the expansion of the arctic ice cap) and the evolution and retreat of the Paratethys Sea have undoubtedly played an important role in the formation and intensification of inland aridity in Asia (Sun et al., 2008; Bosbom et al., 2011; Qiang et al., 2011; Miao et al., 2012; Chi et al., 2013; Haider et al., 2013; Bosbom et al., 2014a; Bosbom et al., 2014b; Bosbom et al., 2014c; Li et al., 2014; Sun et al., 2014; Zhang et al., 2015). However, owing to the different sensitivity of different climatic indicators and the sparse of complete and continuous records, the primary driving mechanism for the evolution of inland aridity in Asian is still under debate.

The use of fossil molecules, such as *n*-alkanes, alkanoic acids, alkenones, GDGTs and those derived from specific biological sources, and $\delta^{13}C$ values of TOC to reconstruct paleoclimate has become an important part of molecular stratigraphy (Xie et al., 2003; Fan et al., 2007; Weijers et al., 2007; Wang et al., 2012; Wu et al., 2018; Tian et al., 2019; Wang et al., 2021a; Wang et al., 2021b). Wang et al. (2012) analyzed the *n*-alkanes and *n*-alkan-2-ones of the sediments collected from the Linxia Basin, and proposed that these biomarkers was in agreement with the palynofloras showing significant variations in response to the climate changes and uplift of the Tibetan Plateau at ~8 Ma. Furthermore, Wu et al. (2018) applied the organic carbon isotopes ($\delta^{13}C_{TOC}$) to reveal the ecological response to the Eocene/Oligocene transition in the Lanzhou Basin, and found that the variations of $\delta^{13}C_{TOC}$ responded to the global cooling. All these indicators displayed great potential in paleoclimate reconstruction in inland Asia.

Northwest China is mainly made up of large inland basins, with extra-thick Cenozoic sediments accumulated. The Linxia Basin is one of them and rich in lipids with weak diagenesis, therefore, is an ideal recorder of arid climatic changes. Previous studies have carried out relevant analyses in the Linxia Basin to establish the general framework of paleoclimate evolution, including low-resolution lipid biomarkers (Wang et al., 2012), microbial communities (He et al., 2020), pollen assemblages (Ma et al., 1998). Nevertheless, detailed paleoclimatic characteristics were limited due to the sample resolution. In the present study, on the basis of previous results, we carried out a systematically high-resolution analyses of lipid biomarkers and $\delta^{13}C$ values of TOC of the Maogou sediments in the Linxia Basin, in hope of revealing the process of arid environmental changes and understanding the driving mechanism of the evolution of Asian inland aridity in the late Cenozoic.

GEOLOGICAL SETTING AND CHRONOLOGICAL FRAMEWORK

The Linxia Basin is located on the northeastern edge of the Tibetan Plateau (102°30′–104°E, 35°10′–35°51′N, **Figure 1**). Sedimentary rocks of the Linxia Basin are mainly composed of mudstone and sandstone of fluvial and lacustrine origin (Fang et al., 2003; Zhang et al., 2019). Climatically, the Linxia Basin is now dominated by an arid/semiarid continental climate with mean annual temperature (MAT) of 6.3°C, mean annual precipitation of 537 mm, and mean annual evaporation of 1,198–1745 mm. Rainfall mainly occurs between June and August, generally following a typical monsoon pattern.

The Maogou section in this research is in the central part of the Linxia Basin (**Figure 1**), which is representative of the tertiary red bed. The Maogou section is characterized by continuous sedimentary strata with a total thickness of 443 m. Li (1995) and Fang et al. (2003) have provided a high-resolution paleomagnetic analysis of the Maogou section to establish the chronological framework. Basically, from the bottom to the top of Maogou section, identified as Tala Formation (0–91 m, ~29–21.4 Ma), Zhongzhuang Formation (92–188 m, 21.4–14.7 Ma), Shangzhuang Formation (189–230 m, 14.7–13.1 Ma), Dongxiang Formation (231–313 m, 13.1–7.8 Ma), Liushu Formation (314–376 m, 7.8–6 Ma) and Hewangjia Formation (377–443 m, 6–4.3 Ma), the magnetostratigraphy results indicated that the sediments from the Maogou section deposited continuously from 29 to 4.3 Ma, spanning from the upper Oligocene to the Pliocene. It is also should be pointed out that there were abundant mammalian fossils which can serve as clear indications of chronology (Deng et al., 2004; Deng et al., 2013). Consequently, the chronological framework was established reasonably and precisely.

SAMPLING AND EXPERIMENTS

Sampling

Actually, our sediment samples were collected from the same section as Li (1995) and Fang et al. (2003) proposed. In order to get the fresh and uncontaminated sediments, an exploratory trench (0.5 m deep and wide) was dug. And then a total of 229 unweathered sediment samples were collected from the trench from the bottom to the top of the Maogou section, from the Tala Formation to the Hewangjia Formation, generally with the sampling interval of 2 m. Most of the samples were composed of silt sandstones, mudstones. All the sediment samples were marked with thickness and stored at -20 C for further analyses.

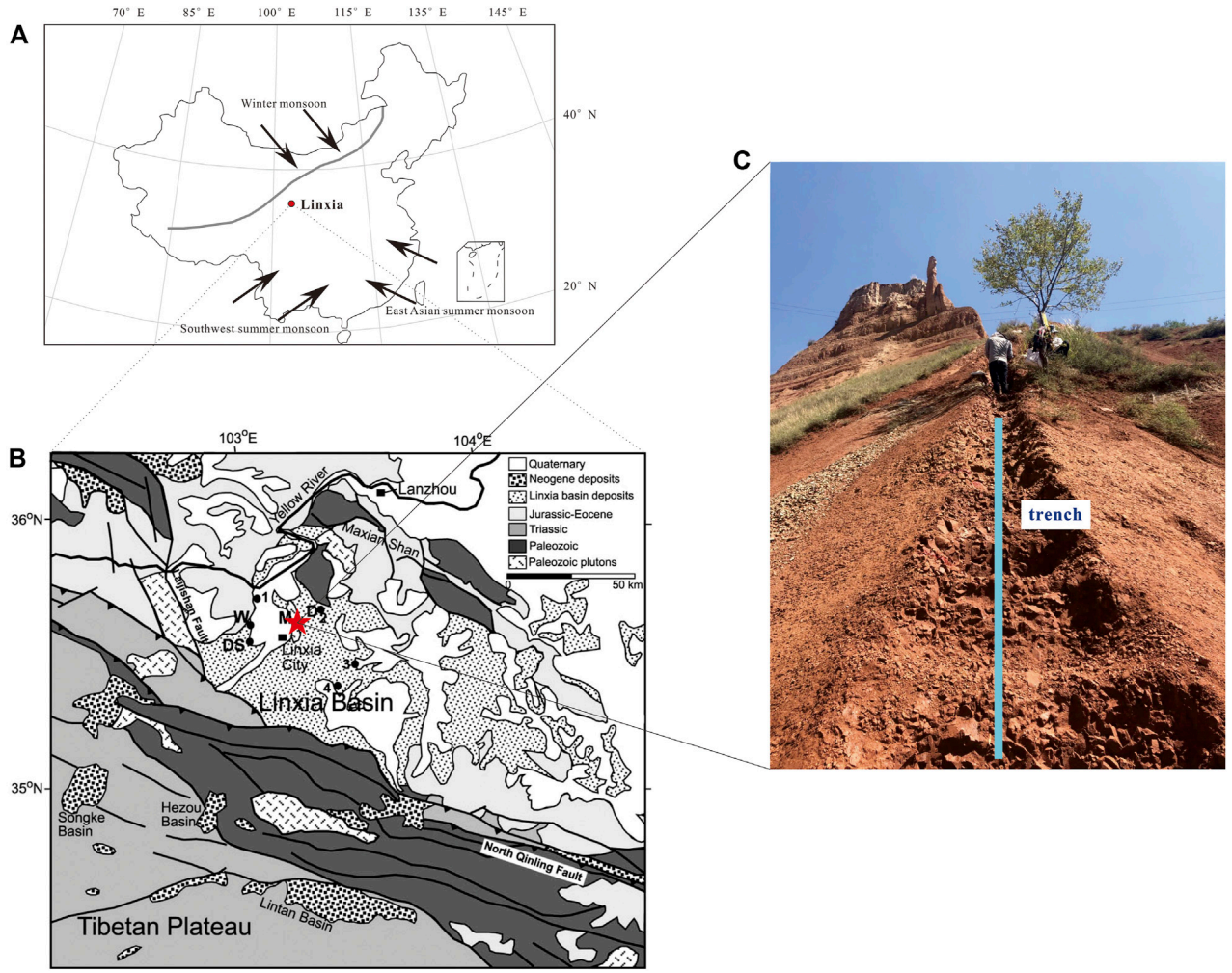

FIGURE 1 | (A) Location of the Linxia Basin (red circle) and the arrow indicating the present main climate controls of China, including southwest summer monsoon, east Asian summer monsoon and winter monsoon (modified from Shao et al. (2006)) **(B)** Simplified geological map of the Linxia Basin. Red pentacle representing the Maogou section (cited from Fang et al., 2003) **(C)** outcrop photograph of the Dongxiang Formation of the Maogou section.

Sample Pretreatment and GC-MS Analysis

The samples (150 g each) were powdered (80 mesh) and extracted with dichloromethane/methanol (93:7) in a Soxhlet extractor for 70 h, and the solvent was removed by distillation. The extracts were condensed and weighed. Because the extracted material was only 1–5 mg, fractionation using chromatography on silica gel or alumina was avoided to prevent the potential loss of components such as the trace alkanes and the oxygen compound. After natural air-drying and dilution using chloroform, the total extracts were analyzed directly using GC-MS. The blank samples were run under similar conditions. The GC-MS spectra of blank samples showed that the lipid molecules to be discussed in this paper were not found.

GC-MS analysis was performed using a HP 5973 MSD interfaced to a HP 6890 gas chromatograph fitted with a 30 m × 0.25 mm i. d. fused silica capillary column coated with a film (0.25 μm) of 5% phenyl-methyl-DB-5. For routine GC analysis, the oven was programmed from 80 to 300°C at 3°C/min with an initial and final hold time of 1 and 30 min, respectively. Helium was used as carrier gas at a linear velocity of 32 cm/s, with the injector operating at a constant flow of 0.9 ml/min. The MS was operated with an ionisation energy of 70 eV, a source temperature of 230°C and an electron multiplier voltage of 1900 V over a range of 35–550 Da.

Carbon Isotopes of Organic Matter ($\delta^{13}C_{org}$)

An aliquot of each sample was acidified with HCl to remove carbonates before analysis. Then, samples were washed with deionized water until a neutral pH value was reached. Next, samples were dried in an oven at 90°C. Pretreated samples were analyzed using a Flash 2000-MAT 253 system. The Flash 2000 was fitted with an oxidation-reduction tube filled with Cr_2O_3, Cu and silver-bearing CoO. Treated samples were oxided at 960°C with flowing oxygen. Helium was used as carrier gas. IAEA-600 (caffeine) was used as standard sample (Coplen et al., 2006). Each sample was analyzed twice, and final

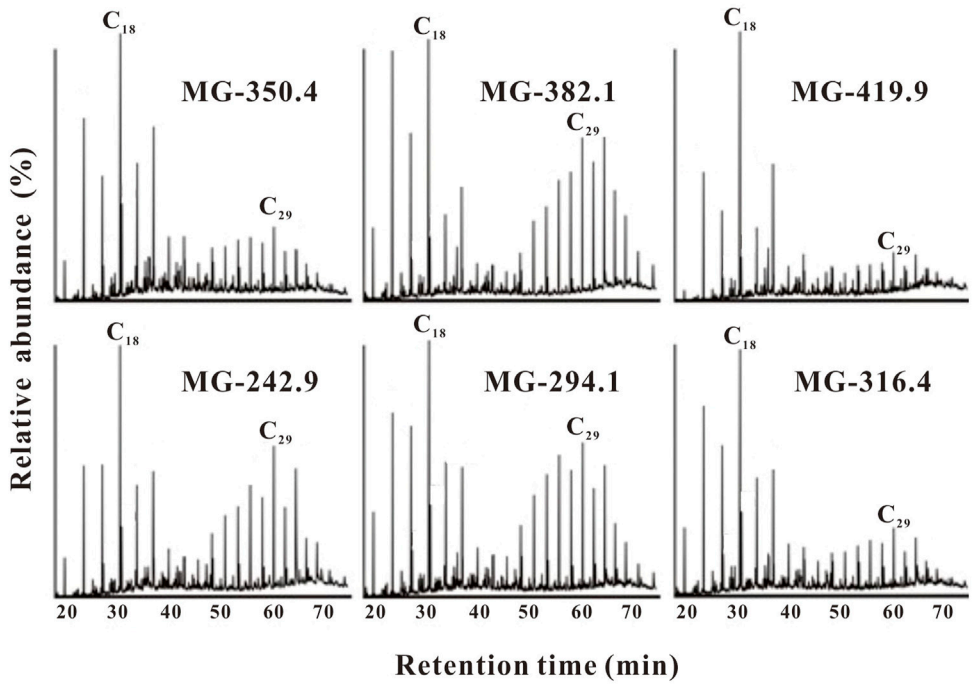

FIGURE 2 | Representative chromatographs of *n*-alkanes (m/z 85) in the Maogou sediments.

averaged results were expressed as ‰ relative to the VPDB (Vienna Peedee Belemnite) standard. During the analysis, 15 standard samples were determined to monitor the accuracy of the instrument. Reproducibility, as determined from the replicate standard samples, were better than 0.05‰ for $\delta^{13}C_{org}$ of organic carbon.

RESULTS

Distribution Patterns of *n*-alkanes, *n*-Alkane-Derived Proxies and Carbon Isotopes of Bulk Organic Matter

Basically, the *n*-alkanes ranges from C_{16} to C_{32} with an obvious maximum carbon number at C_{18} throughout the entire section, characterized by unimodal distribution patterns. Moreover, some samples show a significant bimodal distribution, with C_{18} and C_{29} as the main peaks. A distinct odd-over-even predominance of the long-chain *n*-alkanes is observed throughout the profile. Representative relative abundance of *n*-alkanes from the Maogou section sediments are shown in **Figure 2**.

In terms of the *n*-alkane derived proxies, the ratio of C_{27}/C_{31} and $(C_{17}\text{-}C_{21})/(C_{27}\text{-}C_{31})$ values were calculated in this study. Specifically, the ratio of $(C_{17}\text{-}C_{21})/(C_{27}\text{-}C_{31})$ can be calculated using the following equations:

$$(C_{17}-C_{21})/(C_{27}-C_{31}) = (C_{17}+C_{18}+C_{19}+C_{20}+C_{21})/ \times (C_{27}+C_{28}+C_{29}+C_{30}+C_{31})$$

Besides, the $\delta^{13}C_{org}$ values of the Maogou section sediments varies between -31.0‰ and -22.0‰, with an average value of -26.0‰ (**Figure 3C**).

DISCUSSION

Inputs of Organic Matter

Typically, *n*-alkanes are widely distributed in sedimentary organic matter derived from organisms living in the study area and their catchments, and different compositions of *n*-alkanes can directly reflect different biota (Pearson et al., 2007). Normally, the ratio of $(C_{17}\text{-}C_{21})/(C_{27}\text{-}C_{31})$ of *n*-alkanes can indicate the relative contribution from lower organisms including algae, cyanbacteria, fungi and microbes relative to that from terrestrial higher plants, and thus the corresponding climate conditions (Eglinton and Hamilton, 1967; Cranwell et al., 1987; Rielley et al., 1991; Meyers and Ishiwatari, 1993; Ficken et al., 2000). Besides, the ratio of C_{27}/C_{31} is usually applied to indicate the relative abundance of trees versus grasses, as trees produce high abundance of C_{27} or C_{29} *n*-alkane, while grasses typically generate high C_{31} *n*-alkane. Consequently, a high C_{27}/C_{31} ratio indicates a thrive of trees at the expense of grasses, and thus more contribution from trees to the organic matter (Cranwell et al., 1987).

In our study, abundant *n*-alkanes were detected in all the 229 samples from the Maogou section. Generally, the *n*-alkanes displayed bimodal or unimodal distribution patterns, suggesting that the organic matter were contributed by mixed sources, including lower organisms and terrestrial higher plants.

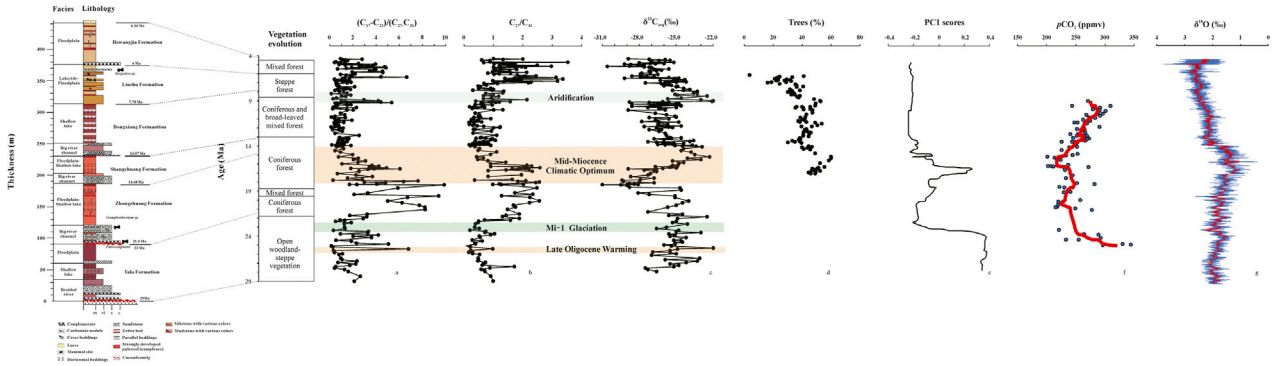

FIGURE 3 | Comparison of different proxies from the Maogou sediments with other indicators, including the ratio of $(C_{17}\text{-}C_{21})/(C_{27}\text{-}C_{31})$ (a), the C_{27}/C_{31} ratio (b), the $\delta^{13}C_{org}$ values of organic matter from Maogou sediments (c), the percentage of tree pollen from the Yanwan section, Tianshui Basin (d) (Hui et al., 2011), the PC1 scores from the Jingou River section in northern Tian Shan, with higher PC1 scores denoting wetter conditions (e) (Tang et al., 2011), the atmospheric CO2 concentrations reconstructed based on the carbon isotopic analyses of diunsaturated alkenones and planktonic foraminifer (f) (Pagani et al., 1999), and the compiled $\delta^{18}O$ records (g) (Westerhold et al., 2020). Further comparison containing the sedimentary facies, lithology, age-depth model modified from He et al. (2020), and vegetation evolution based on pollen records from Ma et al. (1998).

Generally, the ratio of $(C_{17}\text{-}C_{21})/(C_{27}\text{-}C_{31})$ and C_{27}/C_{31} displayed a similar variation trend throughout the sequence (**Figures 3A,B**), indicating the variations of organic matter sources. From 29 to 21.8 Ma, the ratio of $(C_{17}\text{-}C_{21})/(C_{27}\text{-}C_{31})$ and C_{27}/C_{31} remained relatively low-value stage except some fluctuations, suggesting a high proportion of grasses contributed to the organic matter. During the period of 21.8–18 Ma, both the $(C_{17}\text{-}C_{21})/(C_{27}\text{-}C_{31})$ and C_{27}/C_{31} values increased, implying the source of organic matter changed and lower organisms and trees flourished during this interval. From 18 to 14 Ma, the lipid-derived proxies showed a decreasing trend, indicating the sources of trees and lower organisms were limited at this time. Between 14 and 4.3 Ma, our records indicated that the contribution from lower organisms constantly remained constrained, and the abundance of trees slightly increased. According to these observations, we may infer that different organic matter sources at different timescales corresponded to the varying climate conditions.

Paleoclimate Conditions Inferred From $\delta^{13}C_{org}$ and Lipid-Derived Proxies

Terrestrial high plants can normally be divided into three categories, C_3 plants, C_4 plants and CAM plants based on their photosynthesis characteristics and carbon atomicity. C_3 and C_4 plants can be identified according to their carbon isotope values, as C_3 plants are characterized by an $\delta^{13}C$ value ranging from -40‰ to -20‰ with an average of -27‰, and C_4 plants have a distinct $\delta^{13}C$ value between -19‰ and -9‰ with an average value of -12‰, respectively (Smith and Epstein, 1971; Oleary, 1981). It is also generally acknowledged that C_4 plants adapt to an environment which is typical of high temperature, high aridity and low atmospheric CO_2 concentration (Wang and Greenberg, 2007). Particularly, C_4 plants have greater water-use efficiency than C_3 plants (Collatz et al., 1998). In the present study, there is no exact relationship between the $\delta^{13}C_{org}$ values from the Maogou sediments and the reconstructed atmospheric CO_2 concentrations based on the carbon isotopic analyses of diunsaturated alkenones and planktonic foraminifer (Pagani et al., 1999), suggesting the concentration of CO_2 may not be the main factor influencing the vegetation in the Linxia Basin (**Figure 3**). Additionally, previous study indicated that terrestrial higher plants contributed significantly to the organic matter in the sediments in the Linxia Basin (Fan et al., 2007). Consequently, the $\delta^{13}C_{org}$ values may reflect the information of the vegetation communities and its associated climate conditions, such as temperature and/or precipitation (Wang and Deng, 2005; Kohn, 2010; Wu et al., 2018). Overall, the $\delta^{13}C_{org}$ values of the sediments throughout the ~29 to 4.3 Ma varied from -31.0‰ to -22.0‰ (**Figure 3C**), indicating that C_4 grasses were possibly not significant in the Linxia region prior to 4.3 Ma, which is consistent with the conclusion proposed by Fan et al. (2007).

In terms of this background, we attributed the obvious fluctuations of $\delta^{13}C_{org}$ values to the climate variations somewhat arbitrarily, with positive $\delta^{13}C_{org}$ values corresponding to a relatively high abundance of C_4 plants. In the present study, the records of $\delta^{13}C_{org}$ values seemed more sensitive to climate variations as it revealed more stages of climate shifts. From 29 to 21.8 Ma, the $\delta^{13}C_{org}$ values exhibited an overall increasing trend, indicating a relatively high proportion of C_4 plants. Coincidently, the C_{27}/C_{31} ratio displayed a decreasing trend, suggesting an expansion of grasses. As previous study has confirmed that the grasses usually applied the C_4 photosynthesis (Wang and Greenberg, 2007), our results indicated that the vegetation evolution from trees to grasses reflect the vegetation type variations from C_3 to C_4 plants under the relatively warm and dry climate condition (Ao et al., 2021). The pollen assemblages also indicated an open woodland-steppe vegetation mainly composed of *Chenopodipollis,* Polygonaceae, Compositae for the herbs and *Quercoidites, Betulaepollenites, Fraxinoipollenites* and Cupressaceae for the woody plants under a dry condition during this time (Ma et al., 1998). While between 21.8 and 18 Ma, the C_4 grasses shrank while the C_3 trees flourished in this interval, implying a gradual increase in humidity, as indicated by the decreasing $\delta^{13}C_{org}$ values and high C_{27}/C_{31} ratios, corresponding to a

general coniferous forest (Ma et al., 1998). During this interval, the high $(C_{17}\text{-}C_{21})/(C_{27}\text{-}C_{31})$ ratio possibly indicated an increasing contribution from lower organisms to the organic matter. Normally, the $\delta^{13}C_{org}$ of the typical lake algae in fresh water is about −28‰ (Meyers, 1994; Meyers, 2003), thus enhanced inputs of lower organisms may result in negative $\delta^{13}C_{org}$ values in our records. In addition, the sedimentary face was identified as floodplain-shallow lake (Fang et al., 2016), furthering indicating an increasing humidity. Thereafter, a sharp increase in $\delta^{13}C_{org}$ values demonstrated that C_4 grasses increased at the expense of C_3 trees from 18 to 14 Ma, indicating the climate was turning to warm and dry conditions gradually, possibly corresponding to the MMCO (**Figure 3D**) (Zachos et al., 2001; Zan et al., 2015). During this interval, the C_{27}/C_{31} and $(C_{17}\text{-}C_{21})/(C_{27}\text{-}C_{31})$ ratio decreased, suggesting an enhanced contribution from terrestrial higher plants such as grasses and limited inputs of lower organisms, which was in good accordance with the increasing $\delta^{13}C_{org}$ values. The warm and dry climate conditions was beneficial to the growth of grasses. Although this period was recognized as coniferous forest, the percentage of herbs was increasing (Ma et al., 1998). Specifically, the initial stage of the MMCO was characterized by a relatively humid condition as reflected by the proxies, which was also recorded by the pollen assemblages from the northern Tian Shan (Tang et al., 2011) and Linxia Basin (Ma et al., 1998). After the MMCO, the climate was generally dry from 14 to 9.1 Ma, although the humidity showed a slight increase, generally consistent with the vegetation type as coniferous and broad-leaved mixed forest. A rapid increase in $\delta^{13}C_{org}$ values and a sharp decrease in C_{27}/C_{31} and $(C_{17}\text{-}C_{21})/(C_{27}\text{-}C_{31})$ ratio within only less than 1 Ma from 9.1 to 8.5 Ma were observed, suggesting a significantly strengthened aridity at this time under the background of long-term global cooling in the late Cenozoic (Zachos et al., 2001; Westerhold et al., 2020), in accordance with the steppe forest expansion at ~8.5 Ma (Ma et al., 1998). This aridity sustained to ~6.4 Ma and then the humidity displayed a slight increase afterwards. Coincidently, the vegetation evolved towards coniferous and broad-leaved mixed forest, implying the climate became relatively wet (Ma et al., 1998). Considering the refined age-depth model and sample resolution, our records generally agreed with the pollen analysis.

It also should be pointed out that throughout the sequence, the variations of $\delta^{13}C_{org}$ values corresponded well with the changes of lithology basically. This interesting phenomenon was primarily observed in the Dongxiang Formation sediments. The high $\delta^{13}C_{org}$ values occurred when the gray-green clay deposited, and the red bed was characterized by low $\delta^{13}C_{org}$ values. Further studies are necessary to figure out the potential driving mechanisms regarding the frequent fluctuation of the $\delta^{13}C_{org}$ values.

Comparison With Regional and Over-Regional Paleoclimate Records

As mentioned above, our records based on the *n*-alkane-derived proxies and $\delta^{13}C_{org}$ values are overall in good accordance with the pollen records in the Linxia Basin (Ma et al., 1998). Furthermore, the sporopollen records from the Tianshui Basin in the NE Tibetan Plateau demonstrated a temperate, warm-temperate broad-leaved forest between 17.1 and 14.7 Ma, forest or forest-steppe between 14.7 and 11.7 Ma, broad-leaved forest during 11.7–8.5 Ma and steppe vegetation from 8.5 to 6.1 Ma (Hui et al., 2011). Similarly, the sporopollen reports in the Jiuxi Basin revealed a semi-moist climate from 13 to 11.2 Ma, warm and moist climate between 11.2 and 8.6 Ma, warm and semi-moist climate during 8.6–5.6 Ma, semi-arid climate during 5.4–4.9 Ma and arid climate condition in the interval of 4.9–2.2 Ma (Ma et al., 2005). Also, Tang et al. (2011) reported that the climate was wet during the late Oligocene and shifted to dry conditions between 23.8–17.3 Ma, and subsequently ameliorated to a relatively wet stage to 16.2 Ma, but then turned to dry condition until 4.2 Ma and the aridity reached a peak at 13.5 Ma. Despite the lack of long-term comparison of paleoclimate records, our results are in good concert with the periodical reports from previous studies.

Moreover, our reconstructed paleoclimate conditions based on the *n*-alkane-derived proxies and the $\delta^{13}C_{org}$ values exhibited significant variations especially during the typical climate events, which behaved synchronously with previous studies. During the period of ~26 to 25 Ma, our results suggested the grasses expanded, and contributions from trees and lower organisms declined, roughly in association with the late Oligocene Warming (Zachos et al., 2001). Sporopollen records from the Nima Basin indicated that broad-leaved trees increased obviously after 25.6 Ma, in response to the late Oligocene warming, further suggesting the development of south Asian monsoon and accompany of global warming (Wu et al., 2019). At ~23 Ma, the increase of the $(C_{17}\text{-}C_{21})/(C_{27}\text{-}C_{31})$ and C_{27}/C_{31} ratio implied that trees and lower organisms characterized by negative the $\delta^{13}C_{org}$ values increased, leading to the decrease of $\delta^{13}C_{org}$ values from the sediments. This most apparent explanation for the change of organic matter source at ~23 Ma is the Mi-1 Glaciation as revealed by the compiled oxygen isotope records (Zachos et al., 2001). Palynological results from the Xining Basin showed the cold-tolerant conifers shrived while thermophilic plants declined during the Mi-1 Glaciation at ~23 Ma (Miao et al., 2013a). While during the interval of ~18 to 14 Ma, the $(C_{17}\text{-}C_{21})/(C_{27}\text{-}C_{31})$ ratio and C_{27}/C_{31} value were decreasing, while the $\delta^{13}C_{org}$ values exhibited an opposite variation, which suggested that C_4 grasses gradually flourished when the warm and wet climate shifted to warm and dry conditions during the MMCO (Zachos et al., 2001; Westerhold et al., 2020).

The pollen records from both the Tianshui Basin and northern Tian Shan suggested a warm and humid early stage of MMCO turned to warm and dry conditions in the latter periods (Hui et al., 2011; Tang et al., 2011). Moreover, the timing and duration of the MMCO was reported from nearby records as 18–14 Ma in the Qaidam Basin (Miao et al., 2011; Miao et al., 2016) and 17–14 Ma in the Xining Basin (Zan et al., 2015).

Our records demonstrated another significant climate shift at ~9 to 8 Ma. During this period, the $(C_{17}\text{-}C_{21})/(C_{27}\text{-}C_{31})$ and C_{27}/C_{31} value decreased dramatically, and the $\delta^{13}C_{org}$ values of sediments showed a sudden increase within less than 1 Ma, suggesting a prominent plant variation from C_3 to C_4 plants, which was ascribed to the enhanced aridification. Our previous work on *n*-alkan-2-ones and microbial communities from the Maogou section sediments also identified this severe climatic variation (Wang et al., 2012; He et al., 2020). Besides, the pollen

assemblages also indicated an obvious aridification event happened at ~8.5 Ma (Ma et al., 1998). The sporopollen data from the Tianshui Basin recorded a rapid development of steppe at about 8.5 Ma, which suggested a permanent drying of the Asian interior at this time (Hui et al., 2011). Yang et al. (2016) reported that carbonate-derived Sr concentrations and Sr/Ca ratios on the northeastern Tibetan Plateau exhibited weakened chemical weathering intensity and pedogenesis at ~8.6 Ma corresponding to a cold and dry climate linked with the enhanced aridification. Furthermore, stable isotope evidence including the $\delta^{13}C$ and $\delta^{18}O$ values of carbonates and $\delta^{13}C_{org}$ values from the Linxia Basin indicated that the most severe aridity occurred from 9.6 to 8.5 Ma (Fan et al., 2007).

In summary, based on these observations, the reconstructed paleoclimate conditions in the Linxia Basin generally followed the global climate variation trend. Specifically, our records indicated an overall warm and dry period of late Oligocene warming and MMCO, which was in favor of the growth of C_4 grasses, corresponding well with the global climate as revealed by the oxygen isotope records (Zachos et al., 2001; Westerhold et al., 2020). And the dry climate conditions spanning 14–4.3 Ma generally coincided with the global cooling since the expansion of polar ice-sheets at 14 Ma (Zachos et al., 2001). Under this circumstance, the expansion of C_4 grasses at 9–8 Ma cannot be sufficiently explained by the global climate trends. Thus, other possible factors need to be considered. The uplift of the Tibetan Plateau may be responsible for the aridification, as extensive evidence corroborated that the tectonic uplift of the Tibetan Plateau occurred approximately at ~8 Ma (An et al., 2001; Lease et al., 2007; Miao et al., 2012; Yang et al., 2016). The uplift of the Tibetan Plateau resulted in a geographic barrier which blocked moisture transportation from neighboring oceans, leading to an arid continental interior due to the rain shadow effect (Boos and Kuang, 2010), and therefore an enhanced aridification. Moreover, Miao et al. (2012) proposed that the uplift of the TP resulted in the changes of topography, which strongly influenced the moisture pattern in Central Asia during Miocene times, particularly the precipitation rates in the Linxia Basin were significantly affected by the tectonic uplift of the surrounding mountains.

CONCLUSION

In the present study, lipid biomarkers and carbon isotopes of organic matter were analyzed to reconstruct the paleoclimate conditions based on the sediments from the Maogou section, Linxia Basin, northeast TP. Generally, the distribution patterns of *n*-alkanes and its derived proxies indicated that the organic matter of the Maogou section sediments were contributed by mixed sources, including lower organisms like algae, fungi, cyanbacteria and microbes, and terrestrial higher plants. The variations of organic matter sources and evolution of higher plants behaved in accordance with the carbon isotope values $\delta^{13}C_{org}$, serving as good indicators for paleoclimate conditions. Our results clearly demonstrated some typical climatic events, such as the late Oligocene Warming event, MMCO and aridification at ~8.5 Ma. Generally, the paleoclimate conditions in the Linxia Basin were primarily controlled by the global climate variations, but the uplift of the TP was responsible for the aridification event at ~8.5 Ma, which was superimposed on the long-term global cooling.

DATA AVAILABILITY STATEMENT

The original contributions generated for this study are included in the article/supplementary material, further inquiries can be directed to the corresponding author.

AUTHOR CONTRIBUTIONS

GW, YW and ZW contributed conception and design of the study. GW, TZ and XY carried out chemical analysis. WH, XM, TZ and XY contributed to the field work. GW wrote the first draft of the manuscript. All authors contributed to the article and approved the submitted version.

FUNDING

This work was financially supported by the National Natural Science Foundation of China (Grant Nos. 41831176, 41902028, and 41972030), the Second Tibetan Plateau Scientific Expedition and Research (STEP) Program (Grant Nos. 2019QZKK0707), the Chinese Academy of Sciences Key Project (Grant Nos. XDB26020302), the CAS 'Light of West China' Program and the Youth Innovation Promotion Association CAS (No. 2021425).

REFERENCES

An, Z. S., Kutzbach, J. E., Prell, W. L., and Porter, S. C. (2001). Evolution of Asian Monsoons and Phased Uplift of the Himalaya-Tibetan Plateau since Late Miocene Times. *Nature* 411 (6833), 62–66. doi:10.1038/35075035

Ao, H., Liebrand, D., Dekkers, M. J., Zhang, P., Song, Y., Liu, Q., et al. (2021). Eccentricity-Paced Monsoon Variability on the Northeastern Tibetan Plateau in the Late Oligocene High CO_2 World. *Sci. Adv.* 7, eabk2318. doi:10.1126/sciadv.abk2318

Boos, W. R., and Kuang, Z. (2010). Dominant Control of the South Asian Monsoon by Orographic Insulation versus Plateau Heating. *Nature* 463, 218–222. doi:10.1038/nature08707

Bosboom, R. E., Abels, H. A., Hoorn, C., van den Berg, B. C. J., Guo, Z., and Dupont-Nivet, G. (2014a). Aridification in Continental Asia after the Middle Eocene Climatic Optimum (MECO). *Earth Planet. Sci. Lett.* 389, 34–42. doi:10.1016/j.epsl.2013.12.014

Bosboom, R. E., Dupont-Nivet, G., Grothe, A., Brinkhuis, H., Villa, G., Mandic, O., et al. (2014b). Linking Tarim Basin Sea Retreat (West China) and Asian Aridification in the Late Eocene. *Basin Res.* 26 (5), 621–640. doi:10.1111/bre.12054

Bosboom, R. E., Dupont-Nivet, G., Grothe, A., Brinkhuis, H., Villa, G., Mandic, O., et al. (2014c). Timing, Cause and Impact of the Late Eocene Stepwise Sea Retreat from the Tarim Basin (West China). *Palaeogeogr. Palaeoclimatol. Palaeoecol.* 403, 101–118. doi:10.1016/j.palaeo.2014.03.035

Bosboom, R. E., Dupont-Nivet, G., Houben, A. J. P., Brinkhuis, H., Villa, G., Mandic, O., et al. (2011). Late Eocene Sea Retreat from the Tarim Basin (West

China) and Concomitant Asian Paleoenvironmental Change. *Palaeogeogr. Palaeoclimatol. Palaeoecol.* 299, 385–398. doi:10.1016/j.palaeo.2010.11.019

Chi, Y., Fang, X., Song, C., Miao, Y., Teng, X., Han, W., et al. (2013). Cenozoic Organic Carbon Isotope and Pollen Records from the Xining Basin, NE Tibetan Plateau, and Their Palaeoenvironmental Significance. *Palaeogeogr. Palaeoclimatol. Palaeoecol.* 386, 436–444. doi:10.1016/j.palaeo.2013.06.013

Collatz, G. J., Berry, J. A., and Clark, J. S. (1998). Effects of Climate and Atmospheric CO_2 Partial Pressure on the Global Distribution of C_4 Grasses: Present, Past, and Future. *Oecologia* 114, 441–454. doi:10.1007/s004420050468

Coplen, T. B., Brand, W. A., Gehre, M., Groning, M., Meijer, H. A. J., Toman, B., et al. (2006). New Guidelines for Delta 13C Measurements. *Anal. Chem.* 78, 2439–2441. doi:10.1021/ac052027c

Cranwell, P. A., Eglinton, G., and Robinson, N. (1987). Lipids of Aquatic Organisms as Potential Contributors to Lacustrine Sediments-II. *Org. Geochem.* 11, 513–527. doi:10.1016/0146-6380(87)90007-6

Deng, T., Qiu, Z.-X., Wang, B.-Y., Wang, X., and Hou, S.-K. (2013). "Late Cenozoic Biostratigraphy of the Linxia basin, Northwestern China," in *Fossil Mammals of Asia: Neogene Biostratigraphy and Chronology*. Editors X. M. Wang, L. J. Flynn, and M. Fortelius (New York: Columbia University Press), 243–273. doi:10.7312/columbia/9780231150125.003.0009

Deng, T., Wang, X. M., Ni, X. J., and Liu, L. P. (2004). Sequence of the Cenozoic Mammalian Faunas of the Linxia Basin in Gansu, China. *Acta Geol. Sin.* 78, 8–14. doi:10.1111/j.1755-6724.2004.tb00669.x

Eglinton, G., and Hamilton, R. J. (1967). Leaf Epicuticular Waxes. *Science* 156, 1322–1335. doi:10.1126/science.156.3780.1322

Fan, M., Dettman, D. L., Song, C., Fang, X., and Garzione, C. N. (2007). Climatic Variation in the Linxia basin, NE Tibetan Plateau, from 13.1 to 4.3 Ma: The Stable Isotope Record. *Palaeogeogr. Palaeoclimatol. Palaeoecol.* 247, 313–328. doi:10.1016/j.palaeo.2006.11.001

Fang, X., Garzione, C., Van der Voo, R., Li, J., and Fan, M. (2003). Flexural Subsidence by 29 Ma on the NE Edge of Tibet from the Magnetostratigraphy of Linxia Basin, China. *Earth Planet. Sci. Lett.* 210, 545–560. doi:10.1016/S0012-821X(03)00142-0

Fang, X., Wang, J., Zhang, W., Zan, J., Song, C., Yan, M., et al. (2016). Tectonosedimentary Evolution Model of an Intracontinental Flexural (Foreland) basin for Paleoclimatic Research. *Glob. Planet. Change* 145, 78–97. doi:10.1016/j.gloplacha.2016.08.015

Ficken, K. J., Li, B., Swain, D. L., and Eglinton, G. (2000). An N-Alkane Proxy for the Sedimentary Input of Submerged/Floating Freshwater Aquatic Macrophytes. *Org. Geochem.* 31, 745–749. doi:10.1016/S0146-6380(00)00081-4

Haider, V. L., Dunkl, I., Eynatten, H. v., Ding, L., Frei, D., and Zhang, L. (2013). Cretaceous to Cenozoic Evolution of the Northern Lhasa Terrane and the Early Paleogene Development of Peneplains at Nam Co, Tibetan Plateau. *J. Asian Earth Sci.* 70-71, 79–98. doi:10.1016/j.jseaes.2013.03.005

He, W., Wang, G., Wang, Y., Wei, Z., Huang, Z., Zhang, T., et al. (2020). Microbial Communities and Lipid Records of the Linxia Basin, NE Tibetan Plateau: Implications for Enhanced Aridity in the Late Miocene. *J. Asian Earth Sci.* 193, 104290. doi:10.1016/j.jseaes.2020.104290

Hui, Z., Li, J., Xu, Q., Song, C., Zhang, J., Wu, F., et al. (2011). Miocene Vegetation and Climatic Changes Reconstructed from a Sporopollen Record of the Tianshui Basin, NE Tibetan Plateau. *Palaeogeogr. Palaeoclimatol. Palaeoecol.* 308, 373–382. doi:10.1016/j.palaeo.2011.05.043

Jia, G., Bai, Y., Ma, Y., Sun, J., and Peng, P. A. (2015). Paleoelevation of Tibetan Lunpola basin in the Oligocene-Miocene Transition Estimated from Leaf Wax Lipid Dual Isotopes. *Glob. Planet. Change* 126, 14–22. doi:10.1016/j.gloplacha.2014.12.007

Kern, A. K., Kovar-Eder, J., Stachura-Suchoples, K., Wang, W.-M., and Wang, P. (2016). Radiometric Dating Re-Evaluating the Paleoenvironment and Paleoclimate Around the Plio-Pleistocene Boundary in NE China (Changbai Mountains). *Rev. Palaeobotany Palynology* 224, 134–145. doi:10.1016/j.revpalbo.2015.10.002

Kita, Z. A., Secord, R., and Boardman, G. S. (2014). A New Stable Isotope Record of Neogene Paleoenvironments and Mammalian Paleoecologies in the Western Great Plains during the Expansion of C4 Grasslands. *Palaeogeogr. Palaeoclimatol. Palaeoecol.* 399, 160–172. doi:10.1016/j.palaeo.2014.02.013

Kohn, M. J. (2010). Carbon Isotope Compositions of Terrestrial C3 Plants as Indicators of (Paleo)ecology and (Paleo)climate. *Proc. Natl. Acad. Sci. U.S.A.* 107, 19691–19695. doi:10.1073/pnas.1004933107

Kutzbach, J. E., Prell, W. L., and Ruddiman, W. F. (1993). Sensitivity of Eurasian Climate to Surface Uplift of the Tibetan Plateau. *J. Geology.* 101, 177–190. doi:10.1086/648215

Lease, R. O., Burbank, D. W., Gehrels, G. E., Wang, Z., and Yuan, D. (2007). Signatures of Mountain Building: Detrital Zircon U/Pb Ages from Northeastern Tibet. *Geology* 35, 239–242. doi:10.1130/G23057A.1

Li, J., Fang, X., Song, C., Pan, B., Ma, Y., and Yan, M. (2014). Late Miocene-Quaternary Rapid Stepwise Uplift of the NE Tibetan Plateau and its Effects on Climatic and Environmental Changes. *Quat. Res.* 81 (3), 400–423. doi:10.1016/j.yqres.2014.01.002

Li, J. J. (1995). *Uplift of Qinghai-Xizang (Tibet) Plateau and Global Change*. Lanzhou: Lanzhou University Press, 181–207.

Liu, D., Wang, Y., Cheng, H., Edwards, R. L., Kong, X., Wang, X., et al. (2008). A Detailed Comparison of Asian Monsoon Intensity and Greenland Temperature during the Allerød and Younger Dryas Events. *Earth Planet. Sci. Lett.* 272, 691–697. doi:10.1016/j.epsl.2008.06.008

Liu, D., Wang, Y., Cheng, H., Kong, X., and Chen, S. (2013). Centennial-Scale Asian Monsoon Variability during the Mid-Younger Dryas from Qingtian Cave, Central China. *Quat. Res.* 80, 199–206. doi:10.1016/j.yqres.2013.06.009

Liu, W., Yang, H., Wang, H., An, Z., Wang, Z., and Leng, Q. (2015). Carbon Isotope Composition of Long Chain Leaf Wax N-Alkanes in lake Sediments: A Dual Indicator of Paleoenvironment in the Qinghai-Tibet Plateau. *Org. Geochem.* 83-84, 190–201. doi:10.1016/j.orggeochem.2015.03.017

Ma, Y., Fang, X., Li, J., Wu, F., and Zhang, J. (2005). The Vegetation and Climate Change during Neocene and Early Quaternary in Jiuxi Basin, China. *Sci. China Ser. D-Earth Sci.* 48, 676–688. doi:10.1360/03yd0110

Ma, Y. Z., Li, J. J., and Fang, X. M. (1998). The Pollen and Climate Record of Red Bed between 30.6 and 5.0 Ma in the Linxia Basin. *Chin. Sci. Bull.* 43, 301–304.

Manabe, S., and Broccoli, A. J. (1990). Mountains and Arid Climates of Middle Latitudes. *Science* 247, 192–195. doi:10.1126/science.247.4939.192

Meyers, P. A. (2003). Applications of Organic Geochemistry to Paleolimnological Reconstructions: A Summary of Examples from the Laurentian Great Lakes. *Org. Geochem.* 34, 261–289. doi:10.1016/S0146-6380(02)00168-7

Meyers, P. A., and Ishiwatari, R. (1993). Lacustrine Organic Geochemistry-An Overview of Indicators of Organic Matter Sources and Diagenesis in Lake Sediments. *Org. Geochem.* 20, 867–900. doi:10.1016/0146-6380(93)90100-P

Meyers, P. A. (1994). Preservation of Elemental and Isotopic Source Identification of Sedimentary Organic Matter. *Chem. Geology.* 114, 289–302. doi:10.1016/0009-2541(94)90059-0

Miao, Y., Fang, X., Herrmann, M., Wu, F., Zhang, Y., and Liu, D. (2011). Miocene Pollen Record of KC-1 Core in the Qaidam Basin, NE Tibetan Plateau and Implications for Evolution of the East Asian Monsoon. *Palaeogeogr. Palaeoclimatol. Palaeoecol.* 299, 30–38. doi:10.1016/j.palaeo.2010.10.026

Miao, Y., Fang, X., Liu, Y.-S., Yan, X., Li, S., and Xia, W. (2016). Late Cenozoic Pollen Concentration in the Western Qaidam Basin, Northern Tibetan Plateau, and its Significance for Paleoclimate and Tectonics. *Rev. Palaeobotany Palynology* 231, 14–22. doi:10.1016/j.revpalbo.2016.04.008

Miao, Y. F., Fang, X. M., Song, C. H., Yan, X. L., Xu, L., and Chen, C. F. (2013a). Pollen and Fossil wood's Linkage with Mi-1 Glaciation in Northeastern Tibetan Plateau, China. *Palaeoworld* 22, 101–108. doi:10.1016/j.palwor.2013.06.001

Miao, Y. F., Fang, X. M., Wu, F. L., Cai, M. T., Song, C. H., Meng, Q. Q., et al. (2013b). Late Cenozoic Continuous Aridification in the Western Qaidam Basin: Evidence from Sporopollen Records. *Clim. Past* 9 (4), 1863–1877. doi:10.5194/cp-9-1863-2013

Miao, Y., Herrmann, M., Wu, F., Yan, X., and Yang, S. (2012). What Controlled Mid-Late Miocene Long-Term Aridification in Central Asia? - Global Cooling or Tibetan Plateau Uplift: A Review. *Earth-Science Rev.* 112, 155–172. doi:10.1016/j.earscirev.2012.02.003

Miller, K. G., Fairbanks, R. G., and Mountain, G. S. (1987). Tertiary Oxygen Isotope Synthesis, Sea Level History, and Continental Margin Erosion. *Paleoceanography* 2 (1), 1–19. doi:10.1029/PA002i001p00001

Miller, K. G., Wright, J. D., and Fairbanks, R. G. (1991). Unlocking the Ice House: Oligocene-Miocene Oxygen Isotopes, Eustasy, and Margin Erosion. *J. Geophys. Res.* 96 (B4), 6829–6848. doi:10.1029/90JB02015

Molnar, P., Boos, W. R., and Battisti, D. S. (2010). Orographic Controls on Climate and Paleoclimate of Asia: Thermal and Mechanical Roles for the Tibetan

Plateau. *Annu. Rev. Earth Planet. Sci.* 38, 77–102. doi:10.1146/annurev-earth-040809-152456

Oleary, M. H. (1981). Carbon Isotope Fractionation in Plants. *Phytochemistry* 20, 553–567. doi:10.1016/0031-9422(81)85134-5

Pagani, M., Arthur, M. A., and Freeman, K. H. (1999). Miocene Evolution of Atmospheric Carbon Dioxide. *Paleoceanography* 14, 273–292. doi:10.1029/1999PA900006

Pearson, E. J., Farrimond, P., and Juggins, S. (2007). Lipid Geochemistry of Lake Sediments from Semi-Arid Spain: Relationships with Source Inputs and Environmental Factors. *Org. Geochem.* 38, 1169–1195. doi:10.1016/j.orggeochem.2007.02.007

Qiang, X., An, Z., Song, Y., Chang, H., Sun, Y., Liu, W., et al. (2011). New Eolian Red clay Sequence on the Western Chinese Loess Plateau Linked to Onset of Asian Desertification about 25 Ma Ago. *Sci. China Earth Sci.* 54, 136–144. doi:10.1007/s11430-010-4126-5

Quade, J., Cerling, T. E., and Bowman, J. R. (1989). Development of Asian Monsoon Revealed by Marked Ecological Shift during the Latest Miocene in Northern Pakistan. *Nature* 342, 163–166. doi:10.1038/342163a0

Rea, D. K., Snoeckx, H., and Joseph, L. H. (1998). Late Cenozoic Eolian Deposition in the North Pacific: Asian Drying, Tibetan Uplift, and Cooling of the Northern Hemisphere. *Paleoceanography* 13 (3), 215–224. doi:10.1029/98PA00123

Rielley, G., Collier, R. J., Jones, D. M., and Eglinton, G. (1991). The Biogeochemistry of Ellesmere Lake, U.K.-I: Source Correlation of Leaf Wax Inputs to the Sedimentary Lipid Record. *Org. Geochem.* 17, 901–912. doi:10.1016/0146-6380(91)90031-E

Ruddiman, W. F., and Kutzbach, J. E. (1989). Forcing of Late Cenozoic Northern Hemisphere Climate by Plateau Uplift in Southern Asia and the American West. *J. Geophys. Res.* 94, 18409–18427. doi:10.1029/JD094iD15p18409

Shao, X., Wang, Y., Cheng, H., Kong, X., Wu, J., and Edwards, R. L. (2006). Long-Term Trend and Abrupt Events of the Holocene Asian Monsoon Inferred from a Stalagmite $\delta^{18}O$ Record from Shennongjia in Central China. *Chin. Sci. Bull.* 51, 221–228. doi:10.1007/s11434-005-0882-6

Shi, Z., Liu, X., An, Z., Yi, B., Yang, P., and Mahowald, N. (2011). Simulated Variations of Eolian Dust from Inner Asian Deserts at the Mid-Pliocene, Last Glacial Maximum, and Present Day: Contributions from the Regional Tectonic Uplift and Global Climate Change. *Clim. Dyn.* 37, 2289–2301. doi:10.1007/s00382-011-1078-1

Smith, B. N., and Epstein, S. (1971). Two Categories of $^{13}C/^{12}C$ Ratio for Higher Plants. *Plant Physiol.* 47, 380–384. doi:10.1104/pp.47.3.380

Sun, J., Xu, Q., Liu, W., Zhang, Z., Xue, L., and Zhao, P. (2014). Palynological Evidence for the Latest Oligocene–Early Miocene Paleoelevation Estimate in the Lunpola Basin, Central Tibet. *Palaeogeogr. Palaeoclimatol. Palaeoecol.* 399, 21–30. doi:10.1016/j.palaeo.2014.02.004

Sun, J., Zhang, L., Deng, C., and Zhu, R. (2008). Evidence for Enhanced Aridity in the Tarim Basin of China Since 5.3 Ma. *Quat. Sci. Rev.* 27, 1012–1023. doi:10.1016/j.quascirev.2008.01.011

Sun, X., and Wang, P. (2005). How Old Is the Asian Monsoon System?-Palaeobotanical Records from China. *Palaeogeogr. Palaeoclimatol. Palaeoecol.* 222, 181–222. doi:10.1016/j.palaeo.2005.03.005

Tang, Z., Ding, Z., White, P. D., Dong, X., Ji, J., Jiang, H., et al. (2011). Late Cenozoic Central Asian Drying Inferred from a Palynological Record from the Northern Tian Shan. *Earth Planet. Sci. Lett.* 302 (3-4), 439–447. doi:10.1016/j.epsl.2010.12.042

Tian, L., Wang, M., Zhang, X., Yang, X., Zong, Y., Jia, G., et al. (2019). Synchronous Change of Temperature and Moisture over the Past 50 Ka in Subtropical Southwest China as Indicated by Biomarker Records in a Crater lake. *Quat.Sci. Rev.* 212, 121–134. doi:10.1016/j.quascirev.2019.04.003

Wan, S., Clift, P. D., Li, A., Li, T., and Yin, X. (2010). Geochemical Records in the South China Sea: Implications for East Asian Summer Monsoon Evolution over the Last 20 Ma. *Geol. Soc. Lond. Spec. Publications* 342, 245–263. doi:10.1144/SP342.14

Wang, G., Wang, Y., Wei, Z., He, W., Ma, X., and Zhang, T. (2021a). Reconstruction of Temperature and Precipitation Spanning the Past 28 Kyr Based on Branched Tetraether Lipids from Qionghai Lake, Southwestern China. *Palaeogeogr. Palaeoclimatol. Palaeoecol.* 562, 110094. doi:10.1016/j.palaeo.2020.110094

Wang, G., Wang, Y., Wei, Z., He, W., Zhang, T., Ma, X., et al. (2021b). Distribution of *N*-Alkan-2-Ones in Qionghai Lake Sediments, Southwest China, and its Potential for Late Quaternary Paleoclimate Reconstruction. *J. Quat. Sci* 36, 288–297. doi:10.1002/jqs.3271

Wang, H., and Greenberg, S. E. (2007). Reconstructing the Response of C3 and C4 Plants to Decadal-Scale Climate Change during the Late Pleistocene in Southern Illinois Using Isotopic Analyses of Calcified Rootlets. *Quat. Res.* 67, 136–142. doi:10.1016/j.yqres.2006.10.001

Wang, Y., and Deng, T. (2005). A 25 m.y. Isotopic Record of Paleodiet and Environmental Change from Fossil Mammals and Paleosols from the NE Margin of the Tibetan Plateau. *Earth Planet. Sci. Lett.* 236, 322–338. doi:10.1016/j.epsl.2005.05.006

Wang, Y., Fang, X., Zhang, T., Li, Y., Wu, Y., He, D., et al. (2012). Distribution of Biomarkers in Lacustrine Sediments of the Linxia Basin, NE Tibetan Plateau, NW China: Significance for Climate Change. *Sediment. Geology.* 243-244, 108–116. doi:10.1016/j.sedgeo.2011.10.006

Weijers, J. W. H., Schouten, S., van den Donker, J. C., Hopmans, E. C., and Sinninghe Damsté, J. S. (2007). Environmental Controls on Bacterial Tetraether Membrane Lipid Distribution in Soils. *Geochimica et Cosmochimica Acta* 71, 703–713. doi:10.1016/j.gca.2006.10.003

Westerhold, T., Marwan, N., Drury, A. J., Liebrand, D., Agnini, C., Anagnostou, E., et al. (2020). An Astronomically Dated Record of Earth's Climate and its Predictability over the Last 66 Million years. *Science* 369, 1383–1387. doi:10.1126/science.aba6853

Wu, F., Miao, Y., Meng, Q., Fang, X., and Sun, J. (2019). Late Oligocene Tibetan Plateau Warming and Humidity: Evidence from a Sporopollen Record. *Geochem. Geophys. Geosyst.* 20, 434–441. doi:10.1029/2018GC007775

Wu, F., Zhao, Y., Fang, X., and Meng, Q. (2018). An Ecological Response to the Eocene/Oligocene Transition Revealed by the $\delta^{13}C_{TOC}$ Record, Lanzhou Basin, NE Tibetan Plateau. *J. Asian Earth Sci.* 159, 74–80. doi:10.1016/j.jseaes.2018.03.020

Wu, H., Svoboda, M. D., Hayes, M. J., Wilhite, D. A., and Wen, F. (2007). Appropriate Application of the Standardized Precipitation Index in Arid Locations and Dry Seasons. *Int. J. Climatol.* 27 (1), 65–79. doi:10.1002/joc.1371

Xie, S. C., Lai, X. L., Yi, Y., Gu, Y., and Liang, B. (2003). Molecular Fossils in a Pleistocene River Terrace in Southern China Related to a Paleoclimate Variation. *Org. Geochem.* 36 (4), 789–797. doi:10.1016/S0146-6380(03)00026-3

Yang, Y., Fang, X., Galy, A., Jin, Z., Wu, F., Yang, R., et al. (2016). Plateau Uplift Forcing Climate Change Around 8.6 Ma on the Northeastern Tibetan Plateau: Evidence from an Integrated Sedimentary Sr Record. *Palaeogeogr. Palaeoclimatol. Palaeoecol.* 461, 418–431. doi:10.1016/j.palaeo.2016.09.002

Zachos, J., Pagani, M., Sloan, L., Thomas, E., and Billups, K. (2001). Trends, Rhythms, and Aberrations in Global Climate 65 Ma to Present. *Science* 292, 686–693. doi:10.1126/science.1059412

Zan, J., Fang, X., Yan, M., Zhang, W., and Lu, Y. (2015). Lithologic and Rock Magnetic Evidence for the Mid-Miocene Climatic Optimum Recorded in the Sedimentary Archive of the Xining Basin, NE Tibetan Plateau. *Palaeogeogr. Palaeoclimatol. Palaeoecol.* 431, 6–14. doi:10.1016/j.palaeo.2015.04.024

Zhang, R., Jiang, D., Zhang, Z., and Yu, E. (2015). The Impact of Regional Uplift of the Tibetan Plateau on the Asian Monsoon Climate. *Palaeogeogr. Palaeoclimatol. Palaeoecol.* 417, 137–150. doi:10.1016/j.palaeo.2014.10.030

Zhang, W. L., Erwin, A., Wang, J. Y., Fang, X. M., Zan, J. B., Yang, Y. B., et al. (2019). New Paleomagnetic Constraints for Platybelodon and Hipparion Faunas in the Linxia Basin and Their Ecological Environmental Implications. *Glob. Planet. Change* 176, 71–83. doi:10.1016/j.gloplacha.2019.03.002

Zhuang, G., Brandon, M. T., Pagani, M., and Krishnan, S. (2014). Leaf Wax Stable Isotopes from Northern Tibetan Plateau: Implications for Uplift and Climate since 15 Ma. *Earth Planet. Sci. Lett.* 390, 186–198. doi:10.1016/j.epsl.2014.01.003

Conflict of Interest: The authors declare that the research was conducted in the absence of any commercial or financial relationships that could be construed as a potential conflict of interest.